COMMUNICATION

Sensors

ADVANCED
OPTICAL
MATERIALS

www.advopticalmat.de

Electrospun Polymer Fiber Lasers for Applications in Vapor Sensing

Sarah Krämmer,* Fabrice Laye, Felix Friedrich, Christoph Vannahme, Cameron L. C. Smith, Ana C. Mendes, Ioannis S. Chronakis, Joerg Lahann, Anders Kristensen, and Heinz Kalt*

A sensing approach based on laser emissionfrom polymer fiber networks is presented. Poly(methyl methacrylate) (PMMA) fibers doped with a laser dye are fabricated by electrospinning. They form random loop resonators, which show laser emission upon optical pumping. The shift of the spectral position of the narrow lasing modes upon uptake of alcohol vapors (model vapors are methanol and ethanol) serves as sensor signal. Thus, the high sensitivity related to the spectral line shifts of cavity-based transducers can be combined with the fiber's large surface to volume ratio. The resulting optical sensors feature excellent sensing performance due to the large overlap (more than 80%) of light field and transducer. The shift of the laser modes results from the swelling of the polymer when exposed to solvent vapors. Due to distinctly different diffusion coefficients in polymers, the uptake dynamics reflected in the transient shift of the lasing peaks can be used to discriminate ethanol and methanol vapor in mixtures of them. The sensing mechanism is expected to be applicable to other solvent vapors that cause polymer swelling.

Gas and vapor detection is one of the basic sensor applications in environmental monitoring, health care, threat detection, and manufacturing process control. A variety of sensors based on different transduction schemes have been investigated.[1–5]

Dr. S. Krämmer, F. Laye, F. Friedrich, Prof. H. Kalt
Institute of Applied Physics (APH)
Karlsruhe Institute of Technology (KIT)
Wolfgang-Gaede-Str. 1, 76131 Karlsruhe, Germany
E-mail: sarah.kraemmer@kit.edu; heinz.kalt@kit.edu
F. Laye, Prof. J. Lahann
Institute of Functional Interfaces (IFG)
Karlsruhe Institute of Technology (KIT)
Hermann-von-Helmholtz-Platz 1
76344 Eggenstein-Leopoldshafen, Germany
Dr. C. Vannahme, Dr. C. L. C. Smith, Prof. A. Kristensen
Department of Micro- and Nanotechnology
Technical University of Denmark (DTU)
Ørsteds Plads, 2800 Kgs. Lyngby, Denmark
Dr. A. C. Mendes, Prof. I. S. Chronakis
Nano-BioScience Research Group
Technical University of Denmark (DTU)
DTU Food, Søltofts Plads, 2800 Kgs. Lyngby, Denmark
Prof. J. Lahann
Biointerfaces Institute & Chemical Engineering
University of Michigan
Ann Arbor, MI 48109, USA

In particular, polymers have been shown to be sensitive transducers since many of them (e.g., poly(methyl methacrylate) (PMMA) or polydimethylsiloxane (PDMS)) swell upon analyte vapor absorption.[6,7]

Optical sensors taking advantage of the effect of polymer swelling often rely on the change in the optical path length of cavities and thus the resonant wavelength. To this end, the cavities are functionalized with polymers. The swelling has, e.g., been used to deform Fabry–Pérot interferometers.[8] Further, the swelling of polymer coatings of photonic crystals, whispering gallery mode cavities, or optofluidic ring resonators perturbs the light field resulting in a measurable resonance shift upon exposure to analyte vapors.[1,9,10]

Optical sensing using polymers has also been demonstrated for polymer fiber networks which feature a very large surface to volume ratio (10^6 m^{-1}). Such networks are fabricated by electrospinning which is a simple and low-cost technique applicable to a large variety of polymers.[11] Especially light-emitting electrospun fibers are promising since they find applications as, e.g., light sources for lab-on-chip devices, optically pumped lasers,[12–14] and sensors.[15] Detection of metal ions,[16] explosive compounds,[17] and biomolecules[18] with electrospun polymer fibers have been realized using the fluorescence intensity of emitters in the fibers as sensor signal.

In this communication, we present a sensing approach based on laser emission from dye-doped electrospun PMMA fiber networks. The fibers, which were fabricated by mass-production-suitable electrospinning, form random loop resonators that are the origin of lasing emission.[19] Instead of using the fluorescence intensity, the spectral position of the lasing modes serves as sensor signal. Due to the extremely narrow linewidth of the lasing peaks even small shifts in spectral position are detectable.[20] As a result, we can combine the high sensitivity related to the spectral line shifts of cavity-based transducers with the fiber's large surface to volume ratio. The resulting optical sensors feature excellent sensing performance due to the large overlap (more than 80%) of light field and transducer. In contrast to most cavity-based examples presented previously[1,9,10] the polymer is not an external coating but forms the bulk of the transducer. Hence, essentially the complete guided light field experiences the perturbation caused by the analyte molecules.

ADVANCED
SCIENCE NEWS
www.advancedsciencenews.com

ADVANCED
OPTICAL
MATERIALS
www.advopticalmat.de

By performing proof-of-principle experiments with ethanol and methanol vapors, we demonstrate the suitability of the polymer network fiber lasers to detect solvent vapors by exploiting the swelling of the polymer. Since different solvents exhibit distinct diffusion coefficients in polymers, their uptake dynamics are expected to be distinguishable. By analyzing the transient shift of the lasing peaks, we are able to discriminate ethanol and methanol vapor in mixtures of them demonstrating that the diffusion kinetics can be used for identification. We would like to point out that in this work ethanol and methanol serve as model vapors and that the sensing mechanism can also be applied to other solvent vapors that cause polymer swelling.

First, we want to present the origin of the transducer signal and estimate the expected sensitivity. As shown previously, dye-doped polymer fiber networks exhibit lasing emission due to a random distribution of resonators formed during the electrospinning process.[19] The resonators are formed by fibers arranged in loops with sections running in parallel with themselves for a certain distance (see the central loop shown in **Figure 1**a). In this so-called coupling region, light can couple back and forth from one part of the fiber into the other forming a closed optical path. Lasing peaks occur at wavelengths λ fulfilling the resonance condition

$$L \cdot n_{eff} = m \cdot \lambda \tag{1}$$

where L denotes the length of the resonator, n_{eff} the effective refractive index, and m some integer. Fibers not forming a loop cavity only show bare fluorescence. In Figure 1b, an emission spectrum before and during exposure to methanol is shown. Upon exposure to alcohol vapor, the PMMA fibers swell, leading to changes in the optical path length $L \cdot n_{eff}$ of the cavity and therefore resulting in a red-shift of the resonance wavelengths.

The fiber swelling changes both the resonator length L and the effective refractive index n_{eff}, the latter of which is a function of the refractive index of PMMA n_{PMMA} and the fiber radius R.[19] In order to quantify these different contributions, we use results from ellipsometry measurements of thin PMMA films spin-coated on silicon. Both the change in film thickness and the change of the refractive index of PMMA Δn_{PMMA} upon

exposure to ethanol (EtOH) and methanol (MeOH) are evaluated simultaneously. Since the film is fixed to the substrate on one side we assume that the complete volume increment $V \rightarrow V + \Delta V = \alpha \cdot V$ occurs as thickness growth.

To obtain a simple analytical model which predicts the expected shifts of the lasing modes of the loop resonators, the ellipsometry data are transferred to the geometry of the polymer fibers. When extrapolating the data to other concentrations, a linear dependence of the expansion and the change of the refractive index of PMMA on concentration are assumed. Isotropic volume increase of a cylindrical fiber with length $L \rightarrow L + \Delta L = \gamma \cdot L$ and radius $R \rightarrow R + R = \gamma \cdot R$ is connected to the volume increase of the film via

$$\alpha V = V + \Delta V = \pi \cdot \gamma L \cdot (\gamma R)^2 = \gamma^3 V \tag{2}$$

In electrospun fibers, an alignment of the macromolecules is possible which might lead to anisotropic expansion of the fiber. However, since there is no evidence for this, we assumed isotropic expansion for simplicity. Further details on anisotropic expansion can be found in the Supporting Information. The factor α depends on the amount of vapor diffused into the polymer and thus on the alcohol vapor concentration. When $\alpha(\gamma)$ and the change of the refractive index of PMMA during exposure to ethanol or methanol Δn_{PMMA} are known, the shift of the lasing mode can be calculated

$$\frac{\Delta \lambda}{\lambda} = \frac{\Delta L}{L} + \frac{\Delta n_{eff}}{n_{eff}} = (\gamma - 1) + \frac{\Delta n_{eff}(\Delta R) + \Delta n_{eff}(\Delta n_{PMMA})}{n_{eff}} \tag{3}$$

The dependence of the effective refractive index n_{eff} on the refractive index of PMMA n_{PMMA} and on the fiber radius R was determined with finite element method simulations performed with COMSOL. For small changes in fiber radii the model yields comparable results for the lasing peak shifts.

Ellipsometry measurements on PMMA films show that the exposure to ethanol and methanol vapor leads to an increase of the film thickness and to an increase of the refractive index of PMMA. The latter effect is attributed to alcohol molecules filling up holes in the PMMA host matrix. In **Figure 2**, the expected shifts for different ethanol and methanol concentrations are presented and divided into the different contributions. It is clear that the change of the refractive index of PMMA Δn_{PMMA} and the change of the cavity length ΔL are the main contributors to the shift. The effect from a change in radius leading to a change of the effective refractive index is negligible.

To investigate the optical sensing properties of polymer fiber networks lasers we used a micro-photoluminescence setup combined with a vapor mixing system. During the sensing experiments the fiber networks are pumped with excitation energies of about 175 nJ per pulse and the spot size was ≈0.039 mm² resulting in a pump fluence of 450 µJ cm². This is well above the lasing thresholds of the cavities used for
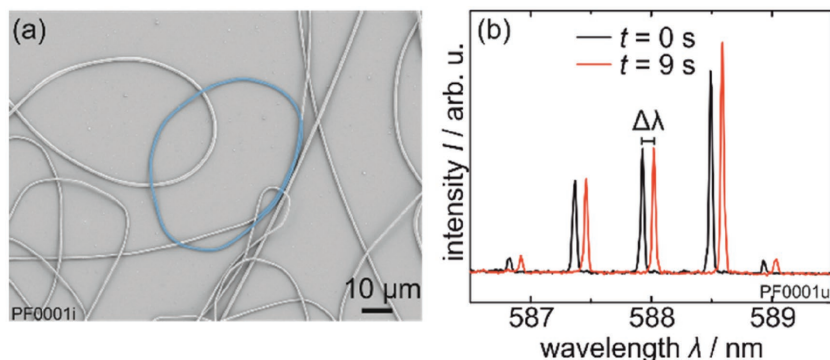

Figure 1. a) Scanning electron microscopy (SEM) image of a PMMA fiber network including a typical loop resonator (marked in blue) responsible for lasing emission. b) Emission spectrum of a resonator before $t = 0$ s (black) and after $t = 9$ s (red) exposure to methanol vapor. The red-shifts of the lasing peaks are clearly visible.

**ADVANCED
SCIENCE NEWS**
www.advancedsciencenews.com
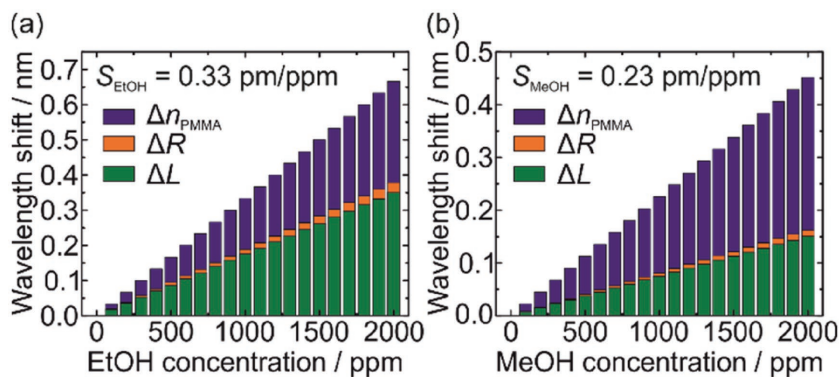
**ADVANCED
OPTICAL
MATERIALS**
www.advopticalmat.de

Figure 2. Expected shifts of the lasing modes when the fibers are exposed to a) ethanol or b) methanol vapor split into contributions from refractive index changes of PMMA (Δn_{PMMA}), length changes (ΔL), and changes of the fiber radius (ΔR).

sensing - for some cavities thresholds as low as 26.5 μJ cm^2 have been measured (compare Figure S1 in the Supporting Information). Spectra are taken every 9 s, so the position of the lasing peaks can be tracked over time. In order to extract the spectral peak position, a Lorentzian function is fitted to the lasing peaks and the center wavelength is determined. In **Figure 3**a,b, example curves showing the shift of the lasing peaks over time are depicted for different concentrations of ethanol and methanol, respectively. The lasing peaks experience a red-shift as

soon as the fibers are exposed to ethanol or methanol vapor (at 0 s).

When the time dependency of the shifts for ethanol and methanol is compared one clearly recognizes that for methanol, saturation is reached within ≈100 s whereas for ethanol the lasing peaks still show a continuing shift after 5400 s. It is evident from the curves in Figure 3b that the peaks shift back to their original spectral position once the sample chamber is purged with pure nitrogen again. Reversibility is also observed for ethanol, but due to the long times this was not monitored for all concentrations.

As expected, we observe higher total shifts of the lasing peaks when reaching saturation for higher alcohol concentrations. For a quantitative analysis of the data, an exponential fit of the form $\Delta\lambda(t) = A_x (1 - \exp(-t/\tau_x))$ was fitted to each measured curve and the final shift A_x and the characteristic time τ_x, referred to as saturation time, were evaluated. In Figure 3c,d, the shifts in saturation A_x are plotted versus the concentration for ethanol and methanol, respectively. For the investigated concentration range, a linear dependence of the shift on the concentration is observed for methanol, while for ethanol saturation seems to start when the concentration exceeds 800 ppm. The slope of the curve (for ethanol only the linear part is considered) gives the sensitivity of the polymer fibers toward the alcohol vapor. For ethanol, the sensitivity is approximately four times higher than for methanol. The reasons for this are the higher molar volume of ethanol which exceeds that of methanol by a factor 1.4 and the better solubility of PMMA in ethanol than in methanol.[21] The latter effectuates that for the same concentration more ethanol molecules diffuse into the PMMA than for methanol. When taking the resolution of the system into account, which is limited by thermal noise, detection limits of 35 and 135 ppm are achieved for ethanol and methanol, respectively. Concerning ethanol, the achieved detection limit is comparable to the sensing based on the wavelength shift of photonic crystal dye lasers where a response threshold of 50 ppm is reported.[1] We did not find any literature reporting on detection of methanol vapor based on a wavelength shift. However, Das et al. reported a detection limit of ≈150 ppm when monitoring the resistance of core–shell nanocomposites, which is approximately a factor of three lower than the detection limit of the polymer fiber lasers.[22]
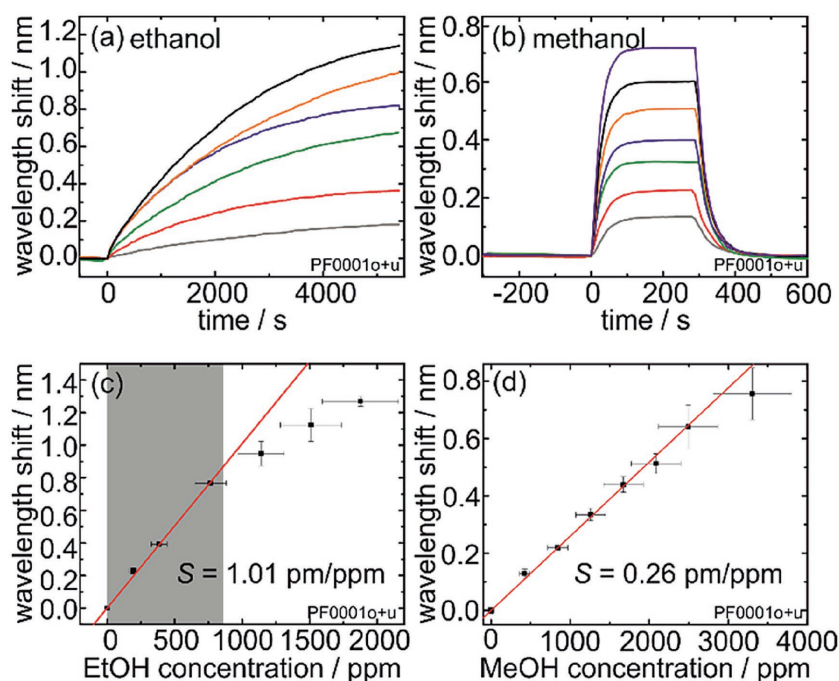
For ethanol, the measured sensitivity exceeds prediction by a factor of three. The reason for this is the linear extrapolation of the ellipsometry data, which were acquired at higher concentrations, to the concentrations used in the sensing experiments, which

Figure 3. a) Typical curves of the time-dependent lasing peak position when the electrospun polymer fibers are exposed to different ethanol concentrations. Concentrations were (from top to bottom) 1880, 1510, 1140, 770, 390, and 190 ppm. b) Time-dependent shift of spectral lasing peak position upon exposure to methanol at concentrations of 3300, 2490, 2080, 1670, 1260, 840, and 420 ppm (from top to bottom). Average shift in saturation for different c) ethanol and d) methanol concentrations. The slope of a linear regression yields the sensitivity. The uncertainty in the concentration was estimated to be 15% due to mixing system. The error bars in y-direction illustrate the standard deviation of different measurements.

**ADVANCED
SCIENCE NEWS**

www.advancedsciencenews.com

**ADVANCED
OPTICAL
MATERIALS**

www.advopticalmat.de

Table 1. Comparison of sensitivity, saturation time, and diffusion coefficient for ethanol and methanol.

	Ethanol	Methanol
Saturation time [s]	2400 ± 500	32 ± 5
Diffusion coefficient [cm^{-2} s][23]	3×10^{-10}	3×10^{-8}
Predicted sensitivity [pm ppm^{-1}]	0.33	0.23
Measured sensitivity [pm ppm^{-1}]	1.01	0.26

deviates from reality (compare Figure 3c). For methanol, the measured sensitivity agrees well with prediction, indicating that the presented model allows one to estimate the expected shifts of the lasing modes.

As can be seen from the graph depicted in Figure 3a, long measurement durations are required for ethanol. In order to abbreviate the measurement duration, data analysis can be performed differently. When the analyte and its saturation time are known, the analyte concentration can be determined from the slope of the exponential curve at $t = 0$ s, allowing a reduction of the measurement duration to $\approx 10\%$ of the saturation time. For further details, see the Supporting Information.

The saturation time shows no dependence on the concentration for either alcohol. The saturation time for methanol is found to be $\tau_M = 32 \pm 5$ s whereas for ethanol $\tau_E = 2400 \pm 500$ s is measured. The fact that the ethanol saturation time exceeds that of methanol by a factor of 75 can be explained by the diffusion coefficients. In fact, the diffusion coefficients for ethanol and methanol in PMMA are $\approx 3 \times 10^{-10}$ cm^2 s^{-1} and 3×10^{-8} cm^2 s^{-1}, respectively,[23] so their inverse ratio agrees well with the ratio of the saturation times. In **Table 1**, all results are summarized. The data strongly suggest that different alcohols should be distinguishable from their dynamics, even in mixtures.

To verify the latter proposition, the electrospun polymer fibers were exposed to mixtures of ethanol and methanol and again the spectral position of the lasing peaks was tracked over time. In **Figure 4**, an example of the resulting data is presented. An exponential fit with two components is fitted to the data
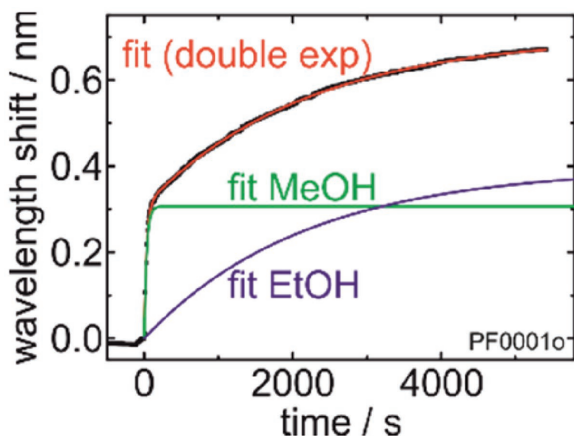

Figure 4. Time-dependent shift of a lasing peak when exposed to a mixture of methanol and ethanol (data from M2, see Table 2). A fast component due to methanol and a slow component due to ethanol diffusion can be clearly identified. An exponential fit with two components represents the data well and yields the saturation times for ethanol and methanol.

Table 2. Mixtures of ethanol and methanol.

	τ_1 [s]	τ_2 [s]	EtOH c_{set}/c_{meas} [ppm]	MeOH c_{set}/c_{meas} [ppm]
M1	3160	49	390/370	420/440
M2	2170	34	390/390	840/1180
M3	2270	42	770/750	420/720

$$\Delta\lambda(t) = A_1\left(1 - \exp(-t/\tau_1)\right) + A_2\left(1 - \exp(-t/\tau_2)\right) \qquad (4)$$

In **Table 2**, the expected and measured values are compared for three different ethanol–methanol mixtures. The times τ_1 and τ_2 can be clearly allocated to the saturation times of ethanol and methanol.

The higher measured saturation times might originate from fibers with higher radius. When the associated shifts in saturation (A_1 and A_2) are translated to concentrations and compared to the set values, good agreement is found for ethanol, while the methanol concentration is overestimated. The excessive values for the methanol concentration, especially for higher ethanol concentrations, lead to the assumption that the presence of ethanol facilitates the diffusion of methanol into PMMA. A similar effect was observed for all-silica decadodecasil 3R crystals, where the presence of water vapor leads to increased absorption of ethanol and methanol.[24] As such, quantification of the methanol concentration in mixtures needs additional calibration. Nevertheless, the presented sensing concept of electrospun polymer fiber networks with lasing emission allows both detection and discrimination of ethanol and methanol.

In summary, we have shown that electrospun polymer fiber networks with lasing emission are suitable as sensors for solvent vapors by using ethanol and methanol as test analytes. The spectral position of the lasing modes serves as sensor signal since it is sensitive to polymer swelling. By developing a simple analytical model and by using results from ellipsometry measurements, we concluded that the shift of the lasing modes upon exposure to alcohol vapors results mainly from changes of the refractive index of PMMA and from length changes of the resonators. Successful detection of ethanol and methanol vapor was demonstrated, revealing saturation times which differ by almost two orders of magnitude due to the different diffusion coefficients of the two alcohols in PMMA. The difference in saturation times allows discrimination of ethanol and methanol when the time-resolved shift is analyzed. Furthermore, we demonstrated that ethanol and methanol vapors can be identified in alcohol mixtures. The presented results serve as proof-of-principle experiments demonstrating that the proposed vapor sensing mechanism, which uses the spectral position of the lasing modes as sensor signal, is working. The sensing mechanism should also work for other solvents that cause polymer swelling and discrimination would be achievable when the solvents exhibit distinct diffusion constants. In future work, polymers other than PMMA, maybe even conjugated polymers as shown by O'Carroll et al.,[25] could be used as additional fiber material, leading to shorter saturation times and enabling differentiation between a greater number of vapors from mixtures.

**ADVANCED
SCIENCE NEWS**

www.advancedsciencenews.com

**ADVANCED
OPTICAL
MATERIALS**

www.advopticalmat.de

Experimental Section

Preparation of Electrospinning Solutions: PMMA (M_W 350 kDa from Sigma-Aldrich) was dissolved in dimetylformamid at ambient temperature with polymer concentration of 12% w/v. The concentration of dye (Pyrromethene 597 from Radiant Laser Dyes) in polymeric spinning solutions was 1.12 mg mL^{-1}. Magnetic stirring was performed for at least 3 h at room temperature in order to obtain homogenously dissolved solutions (the vials were covered with aluminum foil to protect from light).

Electrospinning Processing: A high voltage power supply (ES50P-10W, Gamma High Voltage Research, Inc., USA) was used to provide high voltages in the range of 0–50 kV. To avoid air bubbles, spinning solutions were carefully loaded in a 5 mL syringe to which a stainless steel capillary metal-hub needle was attached. The inside diameter of the metal needle was ≈0.9 mm. The positive electrode of the high voltage power supply was connected to the needle tip. The grounded electrode was connected to a metal collector covered with a 4 in. silicon wafer with a silicon oxide top layer of 200 nm thickness. The silicon oxide ensures that the surface of the substrate is optically transparent, while the silicon serves for conduction. The electrospinning process was carried out at room temperature. A fixed electrical potential of 15 kV was applied across a distance of 20 cm between the tip and the collector. The feed rate of solutions was controlled at 0.05 mL min^{-1} by means of a single syringe pump (New era pump systems, Inc., USA). The resulting polymer fibers had in average a radius of 450 nm. The fabrication process was similar to the one published previously.[19]

Micro-Photoluminescence Setup: For optical excitation of the dye molecules, a frequency-doubled Nd:YVO$_4$ laser emitting pulses of 10 ns at 532 nm with a repetition rate of 20 Hz was used. The laser light was focused on the sample with a lens. The emission light was collected with a microscope objective (50×, NA = 0.42) and guided to a spectrometer equipped with a charged coupled device (CCD) camera. Further information can be found in previous work.[26]

Gas Mixing System: The gas mixing system consisted of three flowmeters and two gas washing bottles filled with ethanol and methanol. Nitrogen served as carrier gas and was guided through the gas washing bottles to obtain saturated ethanol or methanol vapor which was then mixed with pure nitrogen. By adjusting the flow ratios, the desired ethanol or methanol concentration was obtained. The mixture was guided to the sample chamber which was integrated in the optical setup. The sample was placed on a Peltier element to ensure constant temperature during the experiment. A transparent lid made of Plexiglas allowed free space excitation of the fibers and an easy read-out of the lasing emission from the fibers.

Supporting Information

Supporting Information is available from the Wiley Online Library or from the author.

Acknowledgements

Conflict of Interest

The authors declare no conflict of interest.

[1] C. L. C. Smith, J. U. Lind, C. H. Nielsen, M. B. Christiansen, T. Buss, N. B. Larsen, A. Kristensen, *Opt. Lett.* **2011**, *36*, 1392.

[2] S. Some, Y. Xu, Y. Kim, Y. Yoon, H. Qin, A. Kulkarni, T. Kim, H. Lee, *Sci. Rep.* **2013**, *3*, 1868.

[3] B. Ding, M. Wang, J. Yu, G. Sun, *Sensors* **2009**, *9*, 1609.

[4] B. Y. Yang, G. A. Turnbull, I. D. W. Samuel, *Adv. Funct. Mater.* **2010**, *20*, 2093.

[5] R. A. Potyrailo, H. Ghiradella, A. Vertiatchikh, K. Dovidenko, J. R. Cournoyer, E. Olson, *Nat. Photonics* **2007**, *1*, 123.

[6] J. N. Lee, C. Park, G. M. Whitesides, *Anal. Chem.* **2003**, *75*, 6544.

[7] J. S. Papanu, D. W. Hess, D. S. Soane (Soong), A. T. Bell, *J. Appl. Polym. Sci.* **1990**, *39*, 803.

[8] R. St-Gelais, G. MacKey, J. Saunders, J. Zhou, A. Leblanc-Hotte, A. Poulin, J. A. Barnes, H. P. Loock, R. S. Brown, Y.-A. Peter, *Sens. Actuators, B* **2013**, *182*, 45.

[9] Y. Sun, S. I. Shopova, G. Frye-Mason, X. Fan, *Opt. Lett.* **2008**, *33*, 788.

[10] S. Mehrabani, P. Kwong, M. Gupta, A. M. Armani, *Appl. Phys. Lett.* **2013**, *102*, 241101.

[11] A. Frenot, I. S. Chronakis, *Curr. Opin. Colloid Interface Sci.* **2003**, *8*, 64.

[12] A. Camposeo, F. Di Benedetto, R. Stabile, A. A. R. Neves, R. Cingolani, D. Pisignano, *Small* **2009**, *5*, 562.

[13] A. J. Das, C. Lafargue, M. Lebental, J. Zyss, K. S. Narayan, *Appl. Phys. Lett.* **2011**, *99*, 263303.

[14] L. Persano, A. Camposeo, P. Del Carro, V. Fasano, M. Moffa, R. Manco, S. D'Agostino, D. Pisignano, *Adv. Mater.* **2014**, *26*, 6542.

[15] A. Camposeo, L. Persano, D. Pisignano, *Macromol. Mater. Eng.* **2013**, *298*, 487.

[16] P. Anzenbacher, F. Li, M. A. Palacios, *Angew. Chem., Int. Ed.* **2012**, *51*, 2345.

[17] Y. Long, H. Chen, Y. Yang, H. Wang, Y. Yang, N. Li, K. Li, J. Pei, F. Liu, *Macromolecules* **2009**, *42*, 6501.

[18] B. W. Davis, N. Niamnont, C. D. Hare, M. Sukwattanasinitt, Q. Cheng, *ACS Appl. Mater. Interfaces* **2010**, *2*, 1798.

[19] S. Krämmer, C. Vannahme, C. L. C. Smith, T. Grossmann, M. Jenne, S. Schierle, L. Jørgensen, I. S. Chronakis, A. Kristensen, H. Kalt, *Adv. Mater.* **2014**, *26*, 8096.

[20] W. Zeng, Y. Du, Y. Xue, H. L. Frisch in *Physical Properties of Polymers Handbook*, (Ed: J. E. Mark), Springer, New York **2007**, pp. 289–303.

[21] I. M. White, X. Fan, *Opt. Express* **2008**, *16*, 1020.

[22] D. Das, P. Choudhury, L. J. Borthakur, I. R. Kamrupi, U. Gogoi, S. K. Dolui, *Sens. Actuators, B* **2014**, *199*, 320.

[23] G. I. Sarser, N. G. Kalinin, *Sov. Mater. Sci.* **1973**, *9*, 610.

[24] J. Kuhn, J. M. Castillo Sanchez, J. Gascon, S. Calero, D. Dubbeldam, T. J. H. Vlugt, F. Kapteijn, J. Gross, *J. Phys. Chem. C* **2010**, *114*, 6877.

[25] D. O'Carroll, I. Lieberwirth, G. Redmond, *Nat. Nanotechnol.* **2007**, *2*, 180.

[26] T. Grossmann, T. Wienhold, U. Bog, T. Beck, C. Friedmann, H. Kalt, T. Mappes, *Light: Sci. Appl.* **2013**, *2*, e82.